

Modified vector control appropriate for synthesis of all-purpose controller for grid-connected converters

Tihomir Čihak dipl.ing., Mladen Puškarić M.Sc.E.E.
KONČAR Electrical Engineering Institute Inc.
Fallerovo šetalište 22, 10002 Zagreb, Croatia

Ph.D., E.E. Željko Jakopović
Faculty of Electrical Engineering and Computing
Unska 3, 10000 Zagreb, Croatia

Abstract— Vector control and its application in power electronic converters, specifically grid connected inverters and rectifiers is well known topic. Numerous books and articles covered many of its problems and features, but mostly in theoretical way, without taking into account limited computing resources of converter control system, real-life system parameters which can differ from the simplified models used in theoretical analysis and appearance of new parameters as a consequence of concatenating converter with other converters, filters, transformers and other elements. Implementation of vector control in real-life converter is therefore not as straightforward as it may seem. Advanced filter and compensation elements can be hard to implement in a DSP system on one hand and simplified control structures can lead to unstable system or one that does not fulfil necessary requirements on the other hand. This article shows several modifications to simple voltage oriented vector control in three-phase grid connected inverter which handles problems which occur due to connection of transformer between the grid and the converter, but also shows that modifications which have been carried out lead to universally applicable vector control system for grid connected converters.

Keywords— power converters, vector control, renewable energy system, power quality, converter simulation model

I. INTRODUCTION

Modern power electronic converters are, non-dependent on the semiconductor switch technology that they use, essentially unfeasible without a fast and precise control system. Many requirements need to be fulfilled, for instance power factor correction requirements and low values of inrush currents in controlled rectifiers, strictly controlled current harmonic composition and fault ride-through capability in grid connected inverters. Such requirements need modern DSP processors, alone or coupled with FPGA devices, to be achievable. Since these devices are in use, numerous problem solving control algorithms have been invented, from DTC (Direct Torque control) to neural network based control algorithms [16]. Although many of them seem to be an ideal solution to particular problem, practical implementation can be problematic or impossible due to limited processing resources. With good compromise between complexity, good performance and ease of tuning one control method imposed itself as default control system for grid connected PWM converters. Vector control, or more specifically voltage oriented vector control, shown generally in Fig. 2, is chosen

based on several positive features it possesses [4]. Although it is basically a simple and well known control method, in practical implementations many problems regularly appear, most of them not explained in literature in detail. This article will show how to easily circumvent problems that arise from connection of three phase transformer between the basic, typically chosen, PWM inverter and grid. Shown solutions are implemented as add-ons in the control structure in that way that the resulting controller can be used as a more general controller, adaptable to different output topologies found in practice. Also, some important notes on the transducer placement are given.

II. PROPOSED CONTROL SYSTEM

Basic idea behind the control system shown further on is to create a system which can be, with the correct transducer placement, used universally, regardless of the number and character of the filter components between the converter power block and the grid. Adaptation to the specific filtering chain shall be done through disabling the unnecessary controller parts by software parameters rather than changing the controller structure altogether. The core of the controller must be fixed and well defined to allow such changes.

Industry trends in converter design favor simplicity and minimization of component number which eventually lead to lower end prices but on the other hand complicate control algorithms. Typical examples are grid connected inverters for renewable energy sources, as for instance central PV inverters. A typical converter design for such application is shown on diagram in Fig. 1. The DC input passes through the protection and switching equipment (1), into the DC link capacitors (2) and switching block (3). For medium to high power converters, semiconductor block is usually of a three IGBT half-bridge design with one or more IGBTs in parallel depending on the required power [14]. Three phase output is then directed to the output filter (4) which can be of L, LC or multistage filter bank type (emphasized with dashed line after the point (D)). Filtering chain can end either with previously mentioned component or another inductor or transformer (5). Converter is connected to the grid through another set of protection and switching equipment. This article uses LC filter terminated with a transformer as an example.

Transducers can be positioned in a number of ways in converter chain [4]. DC measurements are, as shown in Fig. 1, positioned at point (A), with additional DC measurements at (B) if the topology, e.g. three level converters, requires it. On

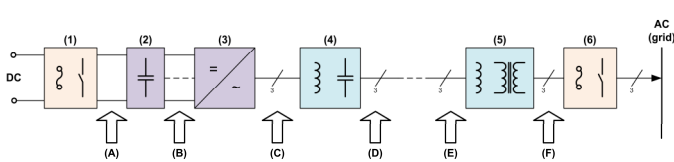


Fig. 1. Converter block diagram.

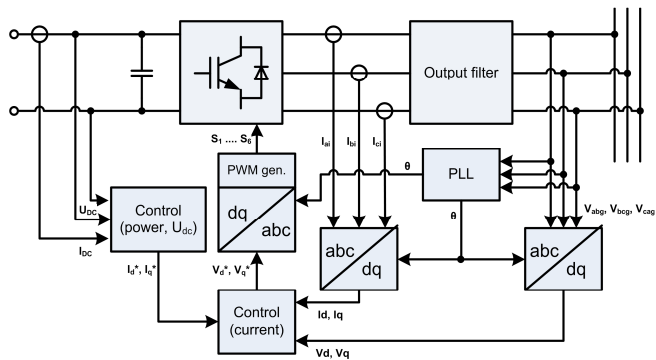


Fig. 2. Block diagram of voltage oriented vector control.

the output side, since correct control of electric variables is required on the interface between the converter and the grid, it would be logical to place transducers at the point (F), but from the controller tuning standpoint [17][18][19], transducers should be placed as close as possible to the (C). In general, positioning current transducers at (C), and voltage transducers at (F) allows for fast current control and the correct estimation of the voltage state in the grid, which makes the control system universal. The downside of this approach is that parameters of all the passive components after the current sensors must be known and compensated for, and any voltage phasor rotation and reduction must be taken into account.

Termination of the converter chain with a transformer differs by a great amount from the typical connection of the converter to the grid directly, through one of filter topologies described in the literature [4][9][15]. This is clearly seen if a converter with a LC filter is connected to the transformer. To explain the influence of the transformer, a variation of a T-model equivalent circuit shown in the Fig. 3 will be used. With transformer at the end of the converter chain, filter topology becomes much more complex, requiring compensation of extra elements. Furthermore, a cross component, transformer magnetization current I_0 occurs and needs to be compensated. Similar current offset components exist on every LC filter node. Parameters required for compensation can be found through simple transformer testing [13]. Also, typical three phase output transformers have phase angle rotation between primary and secondary winding, usually in form of Dy vector group, improving current harmonic content in that way [13] [20]. Such phase rotation needs to be taken into account with proposed current transducer position. In effect, the D and Q current components on the secondary side must be expressed as a sum of the D and Q current components on the primary side if controller topology must not be changed. This is shown in Fig. 4 for D current component only. The same is true for the Q current component.

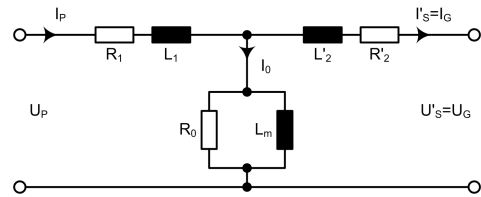


Fig. 3. Used transformer equivalent model.

III. SYNTHESIS OF COMPENSATION BLOCKS

As it can be seen in Fig. 4, power transformers rotate phasors according to their vector group. This is true for both current and voltages. As for the measured voltages, if the transducer position is on point (F) in Fig. 1 this is easily accomplished with fixed angle offset in DQ transformations. According to Fig. 3, a set of equations that describes a transformer and its behavior can be written as:

$$\dot{i}_G = \dot{i}_P - I_0 \quad (1)$$

$$\dot{i}_G = \dot{i}_P - \left(\frac{1}{R_m} u_G + \frac{1}{\omega L_m} u_G \right) \quad (2)$$

$$\dot{i}_P = \dot{i}_{control}; I_{OFF} = \left(\frac{1}{R_m} u_G + \frac{1}{\omega L_m} u_G \right) \quad (3)$$

As the basic requirement on the compensations structure is that the compensation must be added in such way that the basic control structure is not changed, (1) and (2) are rewritten. The controllers are synthesized in DQ system which leads to simple structures essentially controlling DC values. Therefore, an assumption is made that for each operating point the system will reach stationary point at which the output is fixed and directly proportional to the reference value:

$$\dot{i}_{control,comp} (\delta i \approx 0) = \dot{i}_{control} + I_{OFF} \cong I_{REF} + I_{OFF} \quad (4)$$

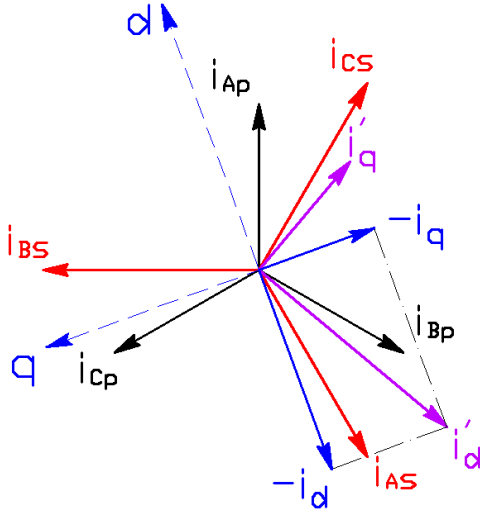
In other words, the exact controller output is not observed, but a known magnetization current is added to the set (reference) current as an offset current. Equations (2) and (4) can now be expressed in DQ system as follows:

$$\dot{i}_{OFFDQ} = \frac{1}{R_m} u_{GDQ} - j \frac{1}{\omega L_m} u_{GDQ} \quad (5)$$

$$\dot{i}_{OFFD} = \frac{1}{R_m} u_{GD} + \frac{1}{\omega L_m} u_{GQ} \quad (6)$$

$$\dot{i}_{OFFQ} = \frac{1}{R_m} u_{GQ} - \frac{1}{\omega L_m} u_{GD} \quad (7)$$

Equations (6) and (7) now show a set of expressions applicable to standard vector control. One distinctive feature of


 Fig. 4. DQ current component coupling on Dy transformer (D component)..

these expressions is the use of the transformed grid side voltages which are known if proposed transducer positions are used. By describing the transformer in this way, compensation can be added as an additional reference component as shown in Fig. 5. Care must be taken when using previous equations; firstly, they imply that the other components prior to the transformer are already compensated. Secondly, an assumption that the transformer can be represented with a set of linear components is made. This will be generally true, but if this is not the case in particular implementation, different methods must be used [12].

The term cross-coupling components assumes control components which negate influence of inductive elements in perpendicular axis [4][21]. In practice, in most of the cases they ignore the influence of filter cross components and the total resistance of components connected to the inverter output. For the cases where capacitor influence can be neglected for a whole multistage filter, these components are defined as:

$$u_{ffD} = u_D - i_Q \cdot (L_1 + \dots + L_n + L_{teqv}) \cdot \omega + i_D \cdot (R_1 + \dots + R_n + R_{teqv}) \quad (8)$$

$$u_{ffQ} = u_Q + i_D \cdot (L_1 + \dots + L_n + L_{teqv}) \cdot \omega + i_Q \cdot (R_1 + \dots + R_n + R_{teqv}) \quad (9)$$

These components are added as feedforward as shown in Fig. 5. If the current flow through transversal filter components can't be neglected, (8) and (9) are not true as the current will change with each consecutive filter stage. Incorporating these influences will require either additional transducers or additional DSP computational capacity. Therefore, for practical implementations, with regard to previous, care must be taken when selecting filtering components. For cases where compensation is still required, but without additional current or voltage transducers, a simple concept can be used.

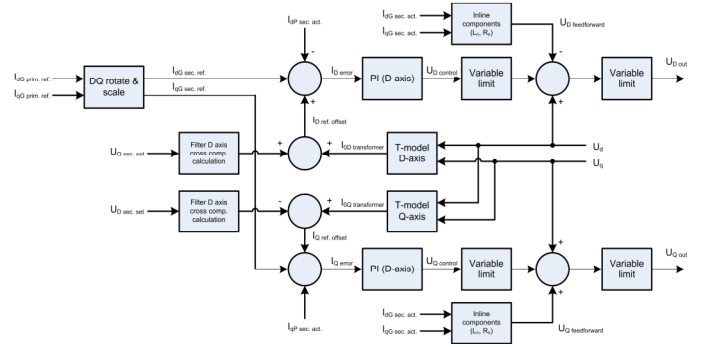


Fig. 5. Block diagram of proposed control system modifications.

For a filtering system that can be approximated as a LCL filter, output current can be expressed as:

$$i_{PCDQ} = i_{PDQ} \cdot (1 - \omega^2 L_1 C) - u_{DQ} \cdot (j\omega C) \quad (10)$$

$$i_{PCD} = i_{PD} \cdot (1 - \omega^2 L_1 C) + u_{setQ} \cdot \omega C \quad (11)$$

$$i_{PCQ} = i_{PQ} \cdot (1 - \omega^2 L_1 C) - u_{setD} \cdot \omega C \quad (12)$$

For special cases, derating expressed in brackets in (10) to (12) can be approximated as:

$$(1 - \omega^2 L_1 C) \approx 1 \quad (13)$$

$$i_{PCD} \cong i_{PD} + u_{setQ} \cdot \omega C \quad (14)$$

$$i_{PCQ} \cong i_{PQ} - u_{setD} \cdot \omega C \quad (15)$$

According to (14) and (15), the current at the second filter stage can be expressed using filter parameters, measured current at the output of the inverter and voltages at the inverter output. These voltages are known from the controller set voltages for the PWM modulation [4][17][19]. By using such compensation, (8) and (9) will necessarily change. Using the known facts on PID controllers [21][22][23], for each operating point, when the system reaches stationary state, current through the first filter component will be equal to the measured current, while at the output of the filter component (input of the next filter stage) current will be equal to the non-compensated reference current expressed in (14) and (15).

IV. IMPLEMENTATION

Developed theoretical groundwork was implemented and tested on a commercial central PV inverter shown in Fig. 6. Inverter is of single stage, grid connected topology with galvanic isolation using output transformer. Inverter is of modular design; it can operate as stand-alone unit or in parallel with identical units on a single transformer for higher output. Testing was done on a stand-alone type. Due to its single-stage topology and control concept with cascaded controllers it proved to be an ideal object for testing of vector control modifications on the grid side part of the control algorithms.



Fig. 6. KonSol-150 central PV inverter.

Control concept allowed disabling algorithm parts that were of no interest for this research without influence on the inverter operation. Some of the technical specifications of the inverter are given in table 1. Control hardware is a custom embedded control system designed as a two-board system. One is a CPU part of the system, and the other is a measurement acquisition and filtering board. The CPU board contains the main DSP coupled with FPGA component and slave DSP. For this research, all algorithm components were implemented in the main DSP. For testing purposes, to avoid misinterpretation of the results, only the grid interface with vector oriented algorithm and grid synchronization with PLL was enabled. To assure correct assessment of the system operation, DC and AC connections with fixed operating points have been provided with a setup shown in Fig. 7. Setup consists of a set of DC generators (only one was used) with output voltage in the range from 0-550V_{DC} and nominal current of 454A_{DC}. In series with generator is a set of adjustable high-power resistors which can be bypassed. Resistors serve as a protection device which limits the maximum input current and to soften the otherwise hard output characteristic of the DC generator. On the AC side, two different sources were used, rotating transformer (3×0-760V_{AC}) for safety reasons, to allow for testing of algorithm at low voltages, and a distribution grid for currents up to 1000A at the connection point. Measurements were done with data acquisition system with external measurement transducers.

V. RESULTS

Several tests were done on the PV inverter to validate the compensation algorithms and investigate the system behavior. Since many protection sequences were disabled to allow for experimentation with the algorithm and inverter parameters, due to safety reasons, operating points under the nominal power were chosen. Input voltage was limited to 500V (open circuit voltage). On the AC side, commissioning was done at half of the nominal voltage and after confirmation of correct operation, testing was done with nominal output voltage. Fig. 8 shows output current and phase voltage for system with compensations. This can be considered reference state for the inverter as it is measured at two thirds of the nominal power

TABLE I. KONSOL-150 TECHNICAL DATA

Absolute maximum input voltage	1000V
MPPT voltage range	410V – 800V
Operational voltage range	380V – 830V
Maximum input current	400A
Nominal power	150kW @ cos φ=1
Nominal voltage	3×380/400V _{RMS}
Nominal current	3×217A _{RMS}

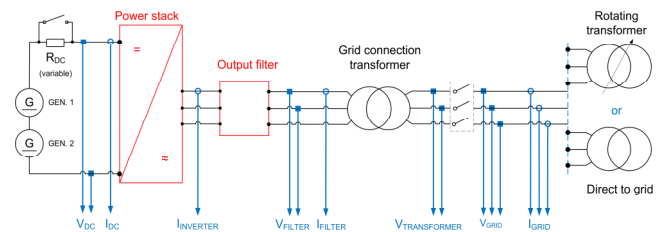


Fig. 7. Inverter measurement setup.

and doesn't change qualitatively up to the nominal inverter power. For a clearer view, picture also shows phasor view of measured values. It is shown directly, as calculated in the data acquisition system, without any post processing. Slight offset (asymmetry) seen on some phasor diagrams is calculation error due to measurement transducer non-ideality, data acquisition processing speed and influence of other loads on the power line. Resulting power factor is shown numerically. A set of tests was done to observe system behavior when transformer parameters are miscalculated. First, system behavior with miscalculation of the transformer model equivalent resistance was observed. Miscalculation was simulated by changing the R_m component value in DSP application into $R_m/4$ and $4 \times R_m$ respectively. Fig. 9 shows power factor changes for this test. As the equivalent resistance enters the compensation calculation as a denominator, power factor does not change linearly. Similar testing was done for the transformer model equivalent magnetizing inductance. Fig. 10 shows resulting changes in power factor. Nonlinear change is observed due to same reasons as in the previous test. Miscalculation was simulated by changing the nominal value of factor $\omega \times L_m$ which is changed into $(\omega \times L_m)/2$ and $(\omega \times L_m) \times 2$ respectively. During both tests no stability problems were found. Next, a throughout evaluation of compensation components, including compensation of transversal filter components was carried out. Testing was done for every combination of algorithm modifications in operating points that were fixed and comparable between tests. Operating points were chosen according to RMS output current. As representative, 25A_{RMS} operating point is shown. Fig. 11 shows output current and phase voltage for system with all compensations (power factor given numerically). Some differences to reference output in Fig. 8 can be observed due to the fact that at chosen operating point inverter is at only 10% of nominal power output. This operating point can be considered worst case for the inverter. This claim supports the fact that most commercial products (central PV inverters) don't have declared values of efficiency, THD and power factor under half of the nominal power. Fig. 12 shows the system state with the transformer compensation disabled, while on the Fig. 13 output filter compensation is disabled. As expected, influence of the transformer compensation is much

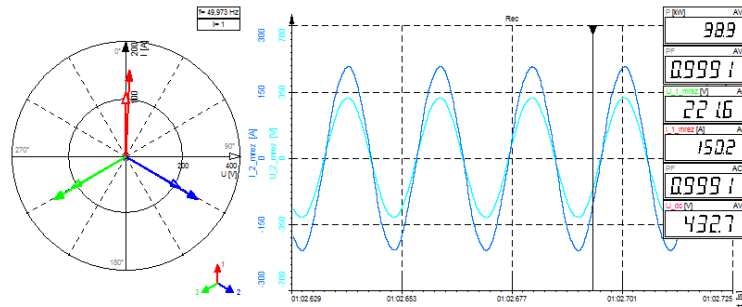


Fig. 8. Inverter output at 150 A_{RMS} with full compensation.

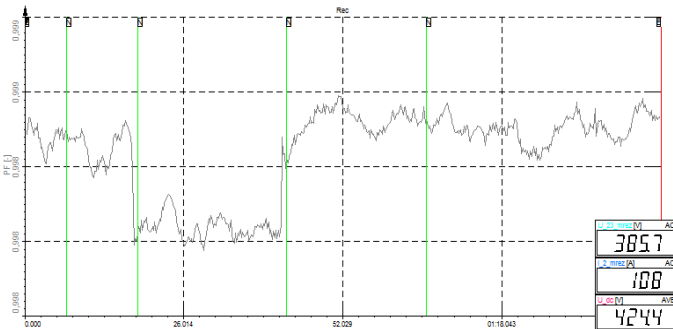


Fig. 9. Power factor change during simulation of R_m miscalculation.

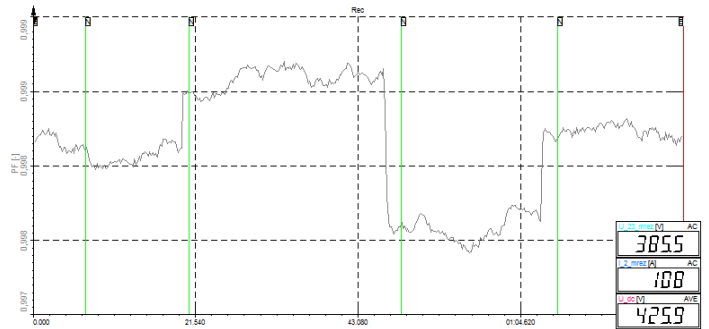


Fig. 10. Power factor change during simulation of $\omega \times L_m$ miscalculation.

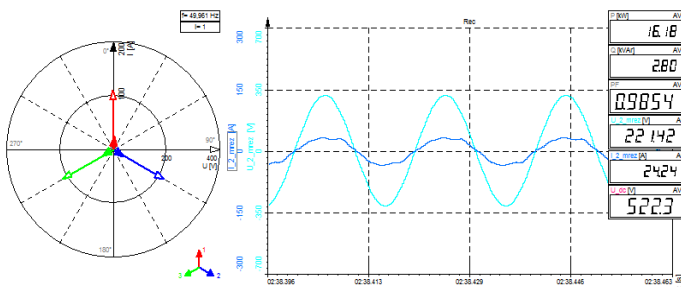


Fig. 11. System with all compensations enabled, 25 A_{RMS} current.

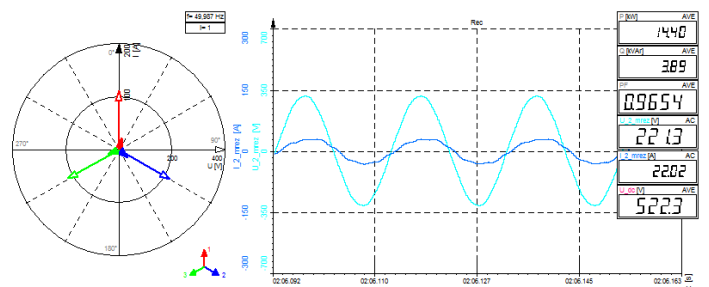


Fig. 12. System with disabled transformer compensation, 25 A_{RMS} current.

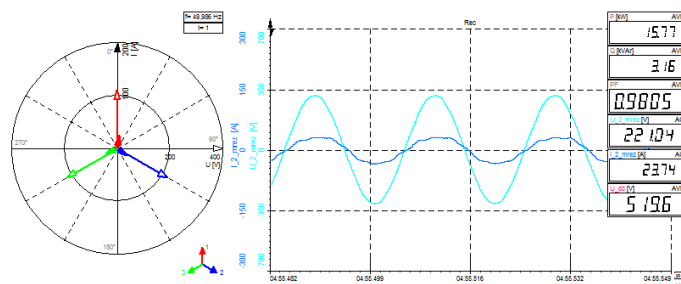


Fig. 13. System with disabled filter offset compensation, 25 A_{RMS} current.

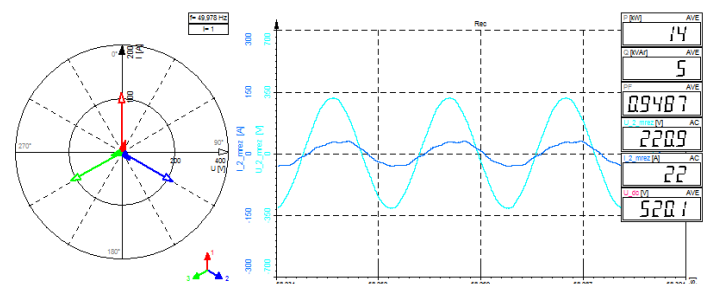


Fig. 14. System with all compensations disabled, 25 A_{RMS} current.

higher than filtering capacitor compensation. But, as results in Fig. 14 show, when all compensation loops are disabled the resulting power factor changes much more than in previous tests. This is due to fact that errors made at the beginning of the controller chain are passed into subsequent control loops and the errors are being magnified and second, under low load system parameters are increasingly non-ideal with more

pronounced nonlinearities in the output. Numerically, compensation loops will change the inner reference currents. For a broader and clearer view on influence of the compensation loops, tests have been made in a wide range, from inverter idle to 80% of the nominal power, with 25 A_{RMS} output current steps. Influence of compensation elements are plotted relative to the non-compensated reference current in

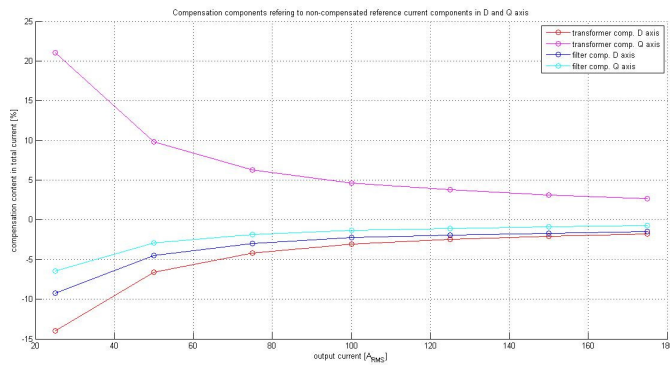


Fig. 15. Compensation amount in percentage referring to non-compensated reference currents in D and Q axis.

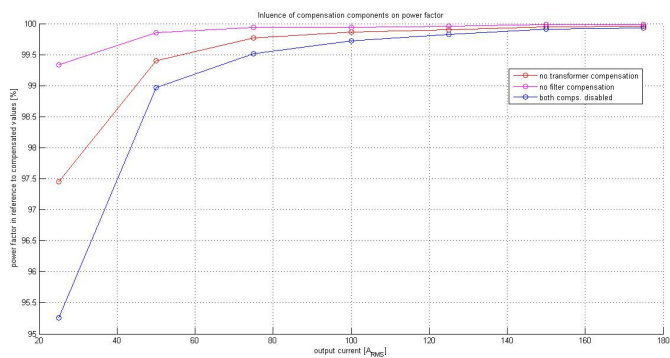


Fig. 16. Power factor change in percentage referring to full-compensation.

Fig. 15. 100% of current is equal to reference currents without compensation. Compensation sign is relative to non-compensated reference. Due to measurement error and transducer noise, measurements under $25A_{RMS}$ are omitted.

VI. CONCLUSION

The assumptions presented at the beginning of this work, that filter and power transformer parameters can be successfully incorporated in the voltage oriented vector control without changing its basic structure are shown through theoretical groundwork which is tested and verified on a real central PV inverter. Presented results show that vector oriented control modifications are successfully implemented and give observable improvement. Also, measured data shows compensation influence throughout the inverter power range. This on one hand shows interdependence of compensation elements and on the other hand it shows in which parts of the inverter power range compensation must be used and parts where approximations used in existing literature are true and can be used safely. Such information, as seen from results, is especially important for power converters that operate at low-load for most of the time, i.e. PV inverters, as current norms suggest [24]. For future work, shown control modifications will be further expanded into compensation system for an arbitrary number of filtering components prior to the output filter or transformer. This expansion will feature reduction of arbitrary number of filtering components into shown structure and automatic parameter determination. This modification will also be implemented and tested on a real inverter.

REFERENCES

- [1] H.-T. Neisius, I. Dzafic, "Three-Phase Transformer Modeling using Symmetrical Components", 17th Power Systems Computation Conference, Stockholm Sweden, August 2011
- [2] J. Dannehl, F.W. Fuchs, S. Hansen, "PWM Rectifier with LCL-Filter using different Current Control Structures", 12th European Conference on Power Electronics and Applications, September 2007, Aalborg, Denmark
- [3] W. H. Kersting, W. H. Phillips, W. Carr, "A New Approach to Modelling Three-Phase Transformer Connections", IEEE Transactions on Industry Applications, vol. 35, no. 1, 1999
- [4] R. Teodorescu, M. Liserre, P. Rodríguez, "Grid Converters for Photovoltaic and Wind Power Systems", John Wiley & Sons, 2011
- [5] M. Reyes, P. Rodríguez, S. Vazquez, A. Luna, R. Teodorescu, J.M. Carrasco, "Enhanced Decoupled Double Synchronous Reference Frame Current Controller for Unbalanced Grid-Voltage Conditions", IEEE Transactions on power electronics, Vol. 27, no.9. September 2012
- [6] Vazquez, G., Kerekes, T., Rocabert, J., Rodríguez, P., Teodorescu, R., Aguilar, D.: A photovoltaic three-phase topology to reduce Common Mode Voltage. Industrial Electronics (ISIE), 2010 IEEE International Symposium on, 4-7 July 2010, pp. 2885 - 2890
- [7] J. Dannehl, C. Wessels, F.W. Fuchs, "Limitations of Voltage-Oriented PI Current Control of Grid-Connected PWM Rectifiers With LCL Filters", Industrial Electronics, IEEE Transactions on, pp. 380 - 388, Feb. 2009
- [8] S.J. Lee, J.K. Kang, S.K. Sul, "A New Phase Detection Method for Power Conversion Systems Considering Distorted Conditions in Power System", IEEE industry applications conference thirty-fourth IAS annual meeting, 1999, vol.4, pp. 2167 - 2172
- [9] J.A. Suul, "Control of Grid Integrated Voltage Source Converters under Unbalanced Conditions", Ph.D. Thesis, Norwegian University of Science and Technology, Trondheim, March 2012
- [10] E. Twining, D.G. Holmes, "Grid Current Regulation of a Three-Phase Voltage Source Inverter With an LCL Input Filter", IEEE Transactions on Power Electronics, vol. 18, no. 3, May 2003
- [11] Y. Yang, Y. Ruan, H. Shen, Y. Tang, "Grid-connected inverter for wind power generation system", Journal of Shanghai University, Volume 13, Issue 1, pp 51-56, February 2009
- [12] B. Terzić, G. Majić, A. Slutej, "Stability Analysis of Three-Phase PWM Converter with LCL Filter by Means of Nonlinear Model", Automatika, vol. 51, no. 3, pp. 221–232, 2010
- [13] A. Dolenc, "Transformatori I i II", Sveučilište u Zagrebu, Elektrotehnički fakultet, Zagreb, 1968
- [14] Infineon: Family documentation - PrimeSTACK, rev 2.3. Infineon Technologies AG, October 2008
- [15] J. Lettl, J. Bauer, L. Linhart, "Comparison of Different Filter Types for Grid Connected Inverter", PIERS Proceedings, Marrakesh, Morocco, March 2011
- [16] F. Jurado, J.R. Saenz, L. Fernandez, "Neural Network Control of Grid-Connected Fuel Cell Plants for Enhancement of Power Quality", IEEE Bologna Power Tech Conference, Bologna, Italy, June 2003
- [17] N. Mohan, T.M. Undeland, W.P. Robbins, "Power Electronics – Converters, Applications and Design", John Wiley & Sons Inc., 2003
- [18] R.C. Dorf, R.H. Bishop, "Modern Control Systems", Pearson Education International, Prentice Hall, 2008, Eleventh Edition
- [19] K.H. Billings, T. Morey, "Switchmode Power Supply Handbook", McGraw-Hill Professional, 2010, Third Edition
- [20] Converter transformers – Part 1: Transformers for industrial applications. IEC 61378-1, Ed. 2.0, 2011-07
- [21] M.P. Kazmierkowski, R. Krishnan, F. Blaabjerg "Control in Power Electronics, Selected Problems", Elsevier Science, Academic Press, 2002
- [22] Z. Vukić, Lj. Kuljača, "Automatsko upravljanje", Kigen, Zagreb, 2005.
- [23] N. Perić, I. Petrović, "Automatsko upravljanje", FER, Zagreb, 2004.
- [24] EN 50530:2010: Overall efficiency of grid connected photovoltaic inverters, CENELEC, 2010